Available online at www.sciencedirect.com
ScienceDirect
Ceramics International 40 (2014) 667–673
CERAMICS INTERNATIONAL
www.elsevier.com/locate/ceramint

Grain growth kinetics of barium titanate synthesized using conventional solid state reaction route

K.R. Kambale, A.R. Kulkarni*, N. Venkataramani

Department of Metallurgical Engineering and Materials Science, Indian Institute of Technology Bombay, Powai, Mumbai 400076, India

Received 11 June 2013; accepted 15 June 2013
Available online 24 June 2013

Abstract

$BaTiO_3$ was synthesized by solid state reaction between $BaCO_3$ and TiO_2 at 1150 °C. XRD analysis of the powder confirmed the formation of phase pure tetragonal powder. The particle size of $BaTiO_3$ powder was of the order of 0.7 μm. In order to study grain growth kinetics of $BaTiO_3$, isothermal sintering was carried out at 1200, 1250 and 1300 °C for the time durations of 2, 4 and 6 h at each of these temperatures. Average grain size increased from 0.4 μm to 1.1 μm on increasing time and temperature of sintering. Corresponding to the temperatures of 1200, 1250 and 1300 °C, grain growth exponents obtained using phenomenological kinetic grain growth equation decreased in the order of 9.77, 4.61 and 3.08 indicating rapid coarsening with increased temperature. Grain growth exponents as high as 4.61 and 9.77 can be regarded as the result of mixed diffusion while grain growth exponent of 3.08 can be the result of pore controlled lattice diffusion. Activation energies calculated in correspondence of grain growth exponents of 9.77, 4.61 and 3.08 were 1307 ± 65, 567 ± 30 and 439 ± 20 kJ/mol respectively.

Keywords: $BaTiO_3$; Phenomenological kinetic grain growth equation; Average grain size; Grain growth exponent; Activation energy

1. Introduction

Barium titanate is a ceramic widely used in electronic industry because of its high dielectric constant and low tangent losses. It is often used as basic ferroelectric material in electronic components such as multilayer ceramic capacitors (MLCC), positive temperature coefficient thermistors (PTC), electro-optic devices, memory applications, sensors and actuators etc. [1]. Traditionally, $BaTiO_3$ is prepared using a high-temperature (>1100 °C) solid-state reaction between $BaCO_3$ and TiO_2 which yields large crystal grains (>3 μm) with a wide range of shape and size. However, these powders result in less chemical homogeneity to such an extent that even if the ratio of $BaCO_3/TiO_2$ is one intermediate phases are retained in end product. On the other hand, wet chemical methods of synthesis such as co precipitation, hydrothermal, micro emulsion and sol gel process offer advantages in terms of processibility, phase purity, homogeneity and controlled stoichiometry but still these methods also pose serious problems. For example, first three methods have complicated washing conditions which are difficult to control. Sol–gel process requires precursors that are highly expensive and are not commonly available. Thus, despite several drawbacks of solid state reaction method, it becomes necessary to study some new aspects of this method because of its amenability to large scale production [2,3]. Barium titanate used in electronic circuits is not in powder form but it is a sintered product with shape formed as per component design. The electrical properties of $BaTiO_3$ are governed by grain size, density, morphology etc. which in turns depend upon grain growth kinetics.

The isothermal rate of grain growth is expressed by phenomenological kinetic grain growth equation:

$$G^n – G_0{}^n = K_0 t \exp(-Q/RT) \tag{1}$$

where G is the average grain size at any time t, G_0 is initial grain size, the n value is kinetic grain growth exponent, K_0 is a pre-exponential constant, Q is the apparent activation energy, R is a universal gas constant and T is the absolute temperature.

---

*Corresponding author. Tel.: +91 22 2576 7636; fax: +91 22 2572 3480.
E-mail addresses: ajit.kulkarni@iitb.ac.in, ajit2957@gmail.com (A.R. Kulkarni).

0272-8842/$ - see front matter © 2013 Elsevier Ltd and Techna Group S.r.l. All rights reserved.
http://dx.doi.org/10.1016/j.ceramint.2013.06.053

When the initial grain size, G_0, is significantly smaller than the average grain size, G, at some later time, then G_0 can be neglected and Eq. (1) can be written as

$$G^n = K_0 t \exp(-Q/RT) \tag{2}$$

Results on grain growth studies, reported in the literature on $BaTiO_3$ are more focussed on primary abnormal grain growth and secondary abnormal grain growth and on microstructural development without considering its kinetics aspects. Grain growth can occur in two different ways namely normal and abnormal. In normal grain growth grain size distribution remains same while during abnormal grain growth a few abnormal grains grow at the expense of fine matrix grains which are often pinned [4]. This abnormal grain growth is often related to the presence of second phase. The $BaTiO_3$–TiO_2 (when TiO_2 is added in excess) system has $BaTiO_3$–$Ba_6Ti_{17}O_{40}$ phase at 1332 °C [5]. This eutectic temperature can vary depending upon inherent impurities present in $BaTiO_3$ powder. When $BaTiO_3$ is sintered above eutectic temperature, primary abnormal grain growth takes place [6,7]. Abnormally large grains nucleate and grow on consuming the fine matrix grains. This grain growth is very rapid and can replace original fine matrix grains with coarser grains in a short period of time. After the grain growth is complete, the microstructure appears to have log normal distribution [8]. If sintering is done between 1360 and 1370 °C, secondary abnormal grain growth sets in. Some of the coarse primary grains begin to grow rapidly and consume other primary grains. This phenomenon is linked to the presence of (111) twins [9,10]. In short, number of research papers discusses the effect of sintering temperature, addition of second phase, oxygen partial pressure, grain boundary faceting, etc. on abnormal grain growth kinetics of $BaTiO_3$ which occurs above eutectic temperature [8,9,11,12]. However, all the reports are silent on diffusion mechanism in terms of grain growth exponent and activation energy. To the best of our knowledge there are no reports in the literature on isothermal rate of grain growth kinetics of $BaTiO_3$ powder synthesized by conventional solid state reaction route. In recent times few attempts have been made to establish grain growth kinetics of nanosized $BaTiO_3$ [13,14] but grain growth kinetics of $BaTiO_3$ synthesized by conventional solid state reaction route has still not been investigated. Therefore, in this study an attempt has been made to establish grain growth exponent and activation energy for isothermal grain growth of $BaTiO_3$ synthesized by conventional solid state reaction route.

2. Experimental

Barium titanate powders were synthesized using barium carbonate ($BaCO_3$) and titania (TiO_2). AR grade micro sized $BaCO_3$ (catalog no: 23710-8) and TiO_2 (catalog no: 232033) were purchased from Aldrich chemical company, USA. Fig. 1 (a) and (b) show SEM micrographs (JEOL JFC-1600 FESEM Oxford Instruments) of micro sized $BaCO_3$ and TiO_2 respectively. It may be noted that the morphology of micro sized (as received) $BaCO_3$ is cylindrical while TiO_2 particles are nearly spherical. Mean particle size of micro sized $BaCO_3$ is 2 μm and TiO_2 is 0.7 μm. In order to determine decomposition temperature of $BaCO_3$, thermo gravimetric analysis (TGA) was carried out (Universal V4 7A TA Instruments). Onset of decomposition temperature of $BaCO_3$ is 825 °C and there occurred 22.46% weight loss during heating up to 1300 °C. This weight loss was considered during batch calculation for synthesizing stoichiometric $BaTiO_3$. The TGA curve for $BaCO_3$ is shown in Fig. 2.

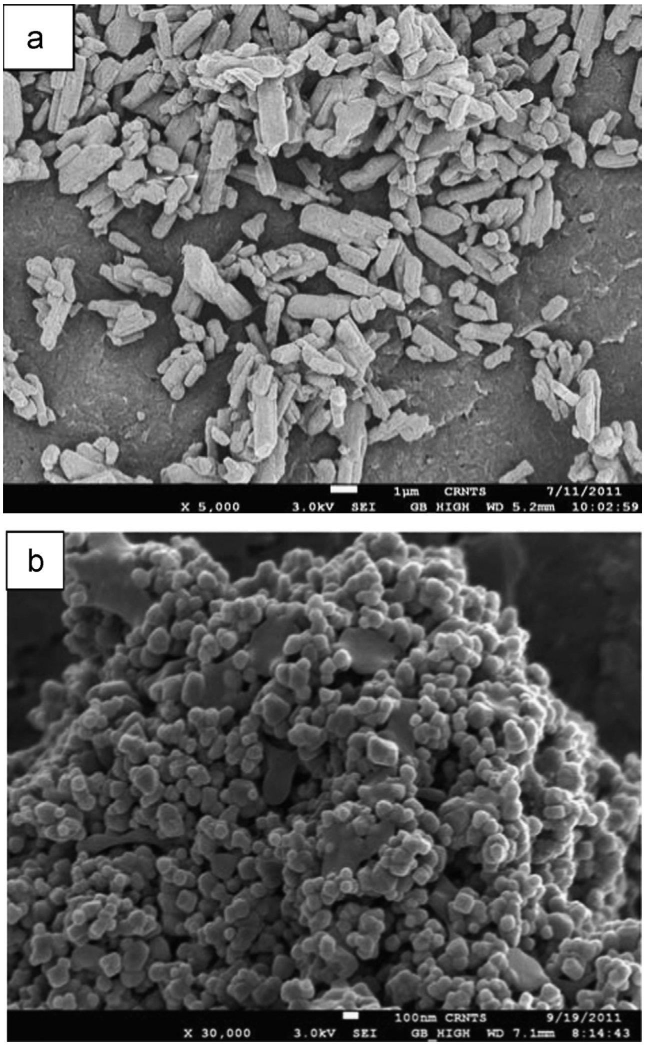

Fig. 1. SEM images of (a) $BaCO_3$ (b) TiO_2.

In order to synthesize barium titanate, starting materials were first mixed in methanol to make slurry and yttria stabilized zirconia balls/powder ratio was kept at 5:1 and the mixture was ball milled for 48 h. The slurry was kept in an oven at 80 °C to evaporate methanol. The dry mass was crushed in agate mortar and pestle to make a fine powder. This powder was calcined at 1150 °C for 4 h. The resultant calcined mass was again crushed in mortar and pestle. To identify the phase of calcined powder, X- ray diffraction was carried out using X-ray diffractometer (PANalytical X-ray diffractometer PW 3040/60) in the 2θ range of 5–90°. X-ray source was Cu-k_α with the wavelength of 1.54 angstrom. Generator voltage

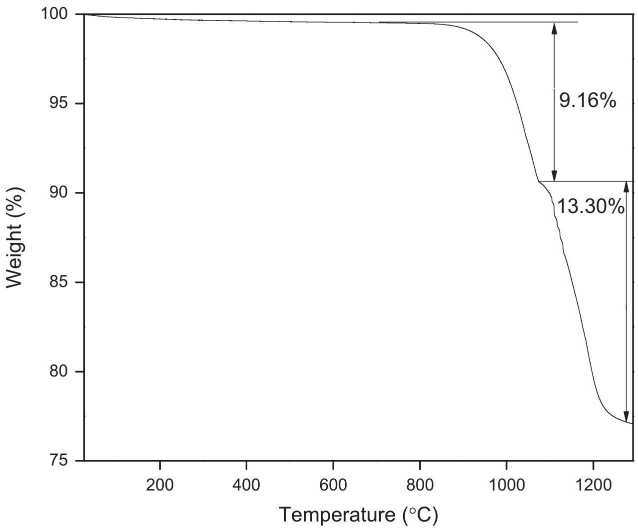

Fig. 2. TGA curve for $BaCO_3$.

and tube current were 40 kV and 30 mA respectively. Room temperature XRD data was collected with a step size of 0.016 and 24.765 s time per step. 3 mol% poly vinyl alcohol (PVA) was added as a binder to calcined powder to give sufficient strength to the green compact. The green density of each pellet was maintained at 57% of theoretical density. The isothermal sintering was carried out at 1200, 1250 and 1300 °C for 2, 4 and 6 h at each of these temperatures. The density of pellets was computed using Archimedes method designated as ASTM C 373-88 [15]. The sintered specimen were successively polished with finer SiC abrasive papers and finally with a diamond paste. The specimens were thermally etched 100 °C below their sintering temperatures before examining the microstructure using SEM (Model Hitachi S3400N) at a magnification of 20,000 × . Grain sizes were directly measured using photomicrographs of these specimens. The average grain size G was obtained by Mendelson's [16] method given as

$$G = 1.56L \tag{3}$$

where, L is the average grain boundary intercept length of a series of random lines on the micrographs.

3. Results and discussion

XRD pattern of $BaTiO_3$ powder synthesized from $BaCO_3$ and micro TiO_2 is shown in Fig. 3. Formation of barium titanate was confirmed with JCPDS database (reference code: 01-079-2264 and ICSD collection code: 067519). Table 1 shows comparison between the calculated and standard parameters of barium titanate powder. It can be seen that actual lattice parameters are in excellent agreement with theoretical lattice parameters and hence, it confirms the formation of tetragonal $BaTiO_3$ powder. Fig. 4 shows SEM micrograph of $BaTiO_3$ powder. It can be seen that this powder has spherical morphology same as of TiO_2 particles. The average particle size is 0.7 μm as confirmed by LASER particle size analyzer.

Table 1
Comparison of lattice parameters of calcined $BaTiO_3$ powder with standard values of lattice parameters of $BaTiO_3$.

Sample	Calculated	Standard	Percentage change
$BaTiO_3$ powder synthesized from $BaCO_3$ and micro TiO_2	$a=3.983$ Å	$a=3.9998$ Å	0.42
	$b=3.983$ Å	$b=3.9998$ Å	0.42
	$c=4.020$ Å	$c=4.0180$ Å	0.0497
	$\alpha=\beta=\gamma=90^\circ$	$\alpha=\beta=\gamma=90^\circ$	0
	$V=63.78$ Å^3	$V=64.28$ Å^3	0.7778

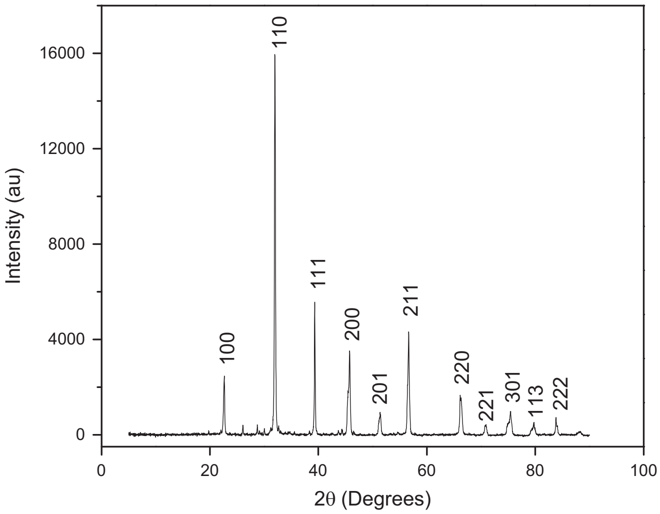

Fig. 3. XRD pattern for calcined $BaTiO_3$ powder.

Table 2
Kinetic parameters for grain growth of $BaTiO_3$.

ln K_0	K_0	n	Q (kJ/mol)
123.34 ± 10.91	3.68×10^{43} ($\mu m^{9.77}$/h)	9.77	1307 ± 65
51.84 ± 6.14	3.26×10^{17} ($\mu m^{4.61}$/h)	4.61	567 ± 30
37.95 ± 3.53	3.03×10^{13} ($\mu m^{3.08}$/h)	3.08	439 ± 20

Fig. 5 shows variation of relative density of $BaTiO_3$ versus sintering time at 1200, 1250 and 1300 °C. With increase in sintering time and temperature, relative density has gradually increased. Sintering at 1200 °C resulted in 81% relative density while maximum density over 99% was achieved at 1300 °C for 4 h of sintering. However, further increasing the sintering time to 6 h at 1300 °C caused decrease in density to 94% which might be attributed to entrapment of gases in pores. The decrease in density after achieving maximum density is a common phenomenon named as swelling or bloating as explained by Rahaman [17] Such kind of behavior of reduction in density after achieving density maximum has been reported in case of isothermal sintering of ZnO [18].

Fig. 6 (a–i) shows SEM micrographs of $BaTiO_3$ sintered at 1200, 1250 and 1300 °C for 2, 4 and 6 h time interval at each of these temperatures. It can be seen from these microstructures that with increasing time and temperature of sintering, grain size has increased gradually from 0.42 μm to 1.1 μm. Moreover, it can be observed that increased time and temperature of

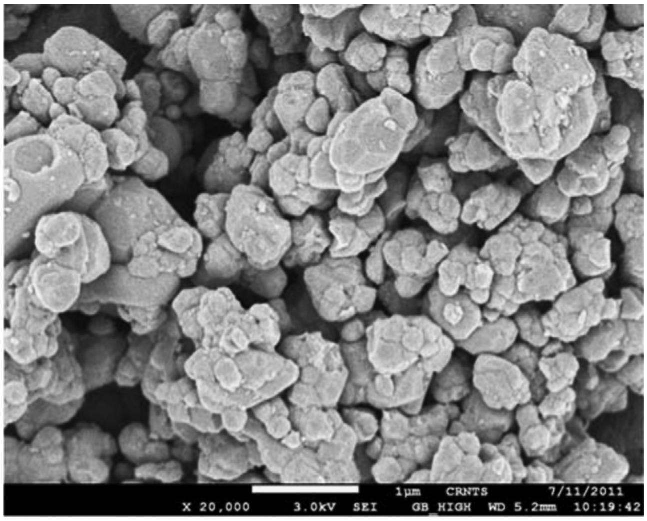

Fig. 4. SEM micrograph of $BaTiO_3$ powder.

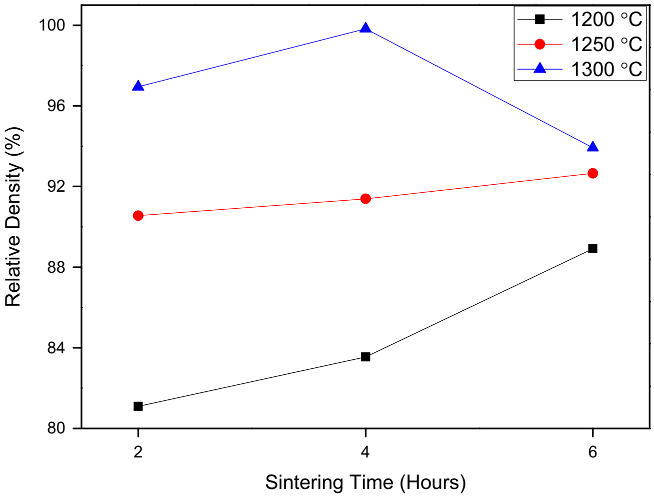

Fig. 5. Variation of relative density of $BaTiO_3$ versus sintering time at 1200, 1250 and 1300 °C.

sintering has caused decrease in porosity. The morphology of $BaTiO_3$ grains is polygonal. Fig. 7 represents variation of average grain size as a function of sintering time at 1200, 1250 and 1300 °C. Average grain size has increased linearly with sintering time at 1200 and 1250 °C and there is a slight deviation from this linearity at 1300 °C. With increasing temperature of sintering, greater driving force was available for grain growth which resulted in increased rate of grain growth with increasing temperature. This increased rate of grain growth has reflected in increased slope of these lines apparent from this graph. At 1200 °C, sintering for 6 h resulted in average grain size of 0.47 µm as compared to average grain size of 0.42 µm for sintering time of 2 h. Average grain size increased from 0.52 µm to 0.66 µm by increasing sintering time from 2 h to 6 h at 1250 °C while it increased from 0.77 µm to 1.1 µm by increasing sintering time from 2 h to 6 h at 1300 °C.

The phenomenological kinetic grain growth equation can be written in the form

$$\ln G = (1/n)\ln t + (1/n)\ln K_0 - (Q/nRT) \tag{4}$$

From the slope of the ln G versus ln t line, which is $1/n$, grain growth exponent can be determined. Fig. 8 illustrates plot of ln G versus ln t at 1200, 1250 and 1300 °C. Values of grain growth exponents are listed in Table 2. It is observed that with increase in temperature from 1200 to 1300 °C, the grain growth exponent decreases from 9.77 to 3.08. The grain growth exponent at 1300 °C, for practical purpose, can be considered to be 3. In theory there are number of mechanisms proposed for grain growth exponent of 3 namely pore controlled lattice diffusion, pore controlled vapor transport (with constant vapor pressure), boundary controlled coalescence of second phase particles for system containing second phase particles and boundary controlled solute drag for doped system [17]. However, system under consideration neither contains second phase particles nor any dopants and hence, diffusion mechanisms listed above for boundary control does not apply. Moreover, sintering has been carried out in solid state and no question arises of vapor transport and thus, it can be safely concluded that at 1300 °C diffusion mechanism is pore controlled lattice diffusion. However, higher values of grain growth exponent of 9.77 and 4.61 at 1200 and 1250 °C cannot simply be explained by a single diffusion mechanism. The diffusion process at these temperatures might have been governed by mixed diffusion mechanisms. Large grain growth exponents are indicative of slowly coarsening microstructures, for the rate of grain growth (dG/dt or $d(\ln G)/d(\ln t)$), decreases with increasing n value, as can be readily seen by differentiating Eq. 4 [19]. Change in values of grain growth exponent with temperature indicating change in diffusion mechanism has been reported in the literature for number of systems [19–21].

If Eq. (2) is expressed in the form of

$$ln\left(\frac{G^n}{t}\right) = ln\ K_0 - \left(\frac{Q}{RT}\right) \tag{5}$$

The apparent activation energy corresponding to grain growth process can be calculated from the gradient of the Arrhenius plot of $\ln(G^n/t)$ versus $10^4/T$. Such plots are shown in Fig. 9 (a–c) corresponding to three values of grain growth exponent. These three values of grain growth exponent yield three equations of the Arrhenius form as follows.

$$ln\left(\frac{G^{9.77}}{t}\right) = ln\ K_0 - \left(\frac{Q}{RT}\right) \tag{6}$$

$$ln\left(\frac{G^{4.61}}{t}\right) = ln\ K_0 - \left(\frac{Q}{RT}\right) \tag{7}$$

$$ln\left(\frac{G^{3.08}}{t}\right) = ln\ K_0 - \left(\frac{Q}{RT}\right) \tag{8}$$

The values of Q and K_0 are summarized in Table 2. There exists a dispersion in the plot of $\ln(G^n/t)$ versus $10^4/t$ at temperatures where grain growth does not correspond to the

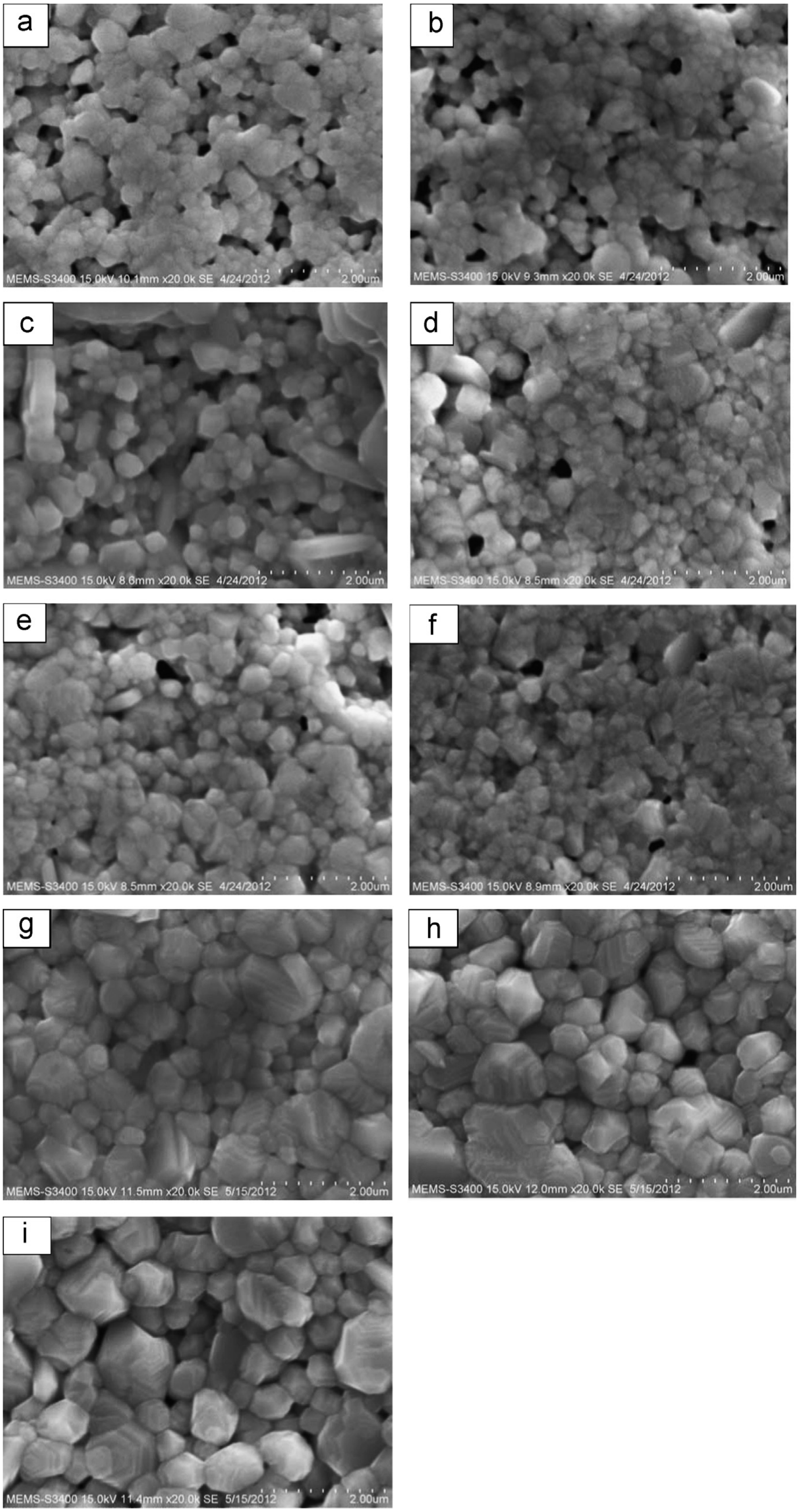

Fig. 6. SEM micrographs of $BaTiO_3$ ceramics sintered at 1200 °C for (a) 2 h (b) 4 h (c) 6 h at 1250° for (d) 2 h (e) 4 h (f) 6 h and at 1300 °C for (g) 2 h (h) 4 h (i) 6 h.

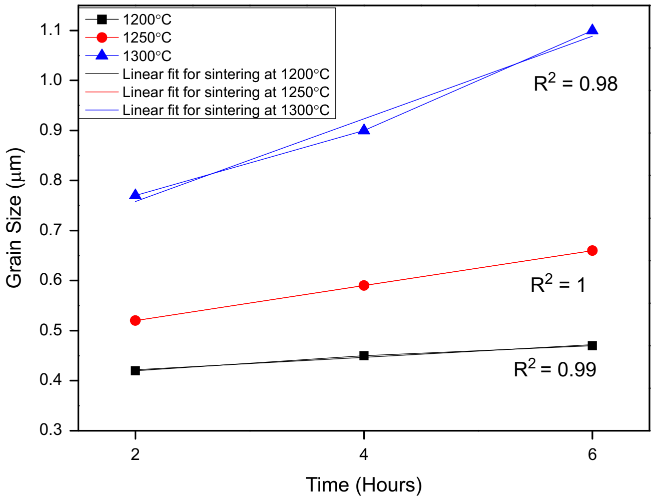

Fig. 7. Variation of average grain size as a function of sintering time at 1200, 1250 and 1300 °C.

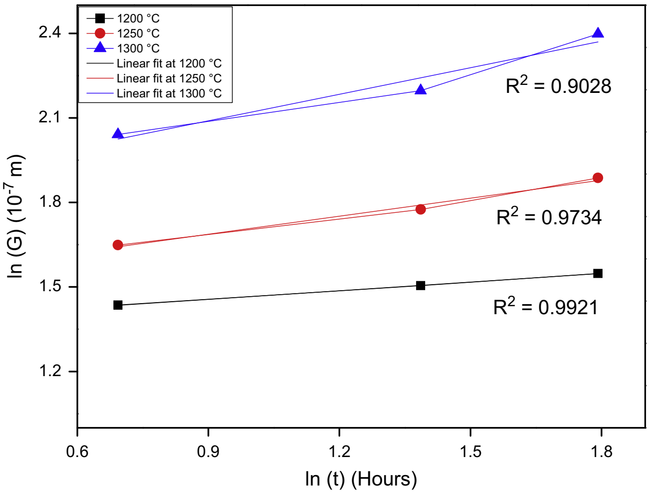

Fig. 8. Plot of ln G versus ln t.

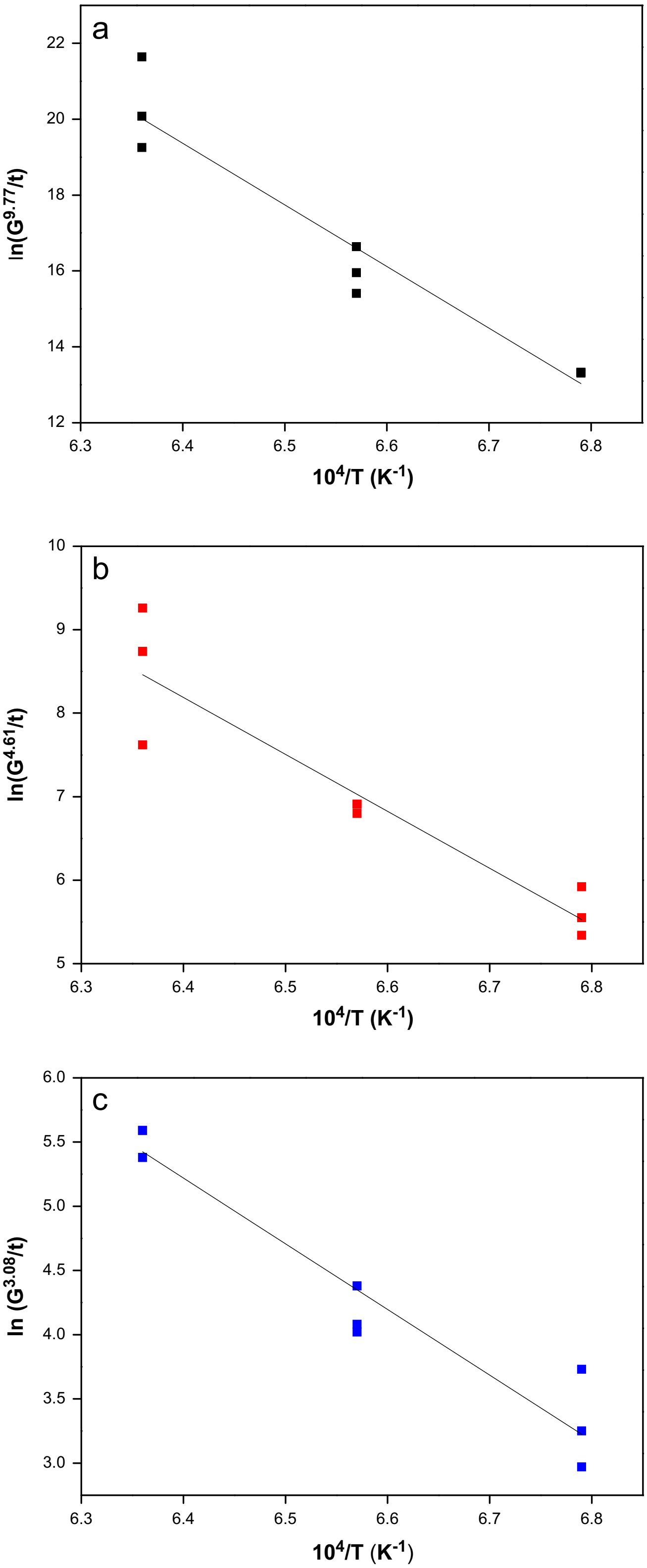

Fig. 9. Arrhenius plots corresponding to grain growth exponents of (a) 9.77 (b) 4.61 and (c) 3.08.

specific value of grain growth exponent. For example, corresponding to grain growth exponent of 9.77, which represents grain growth exponent at 1200 °C, dispersion occurs in the plot of ln($G^{9.77}/t$) versus $10^4/t$ for grain growth at 1250 and 1300 °C. Such dispersion is evident in each such plot and thus, activation energies were calculated by taking best fit (linear) of each of the plot. Corresponding to grain growth exponents of 9.77, 4.61 and 3.08; values of activation energy obtained are 1307 ± 65, 567 ± 30 and 439 ± 20 kJ/mol respectively. Activation enthalpy of diffusion of Ti in $BaTiO_3$ calculated by theoretical model is reported in the literature to be equal to 1458 kJ/mol which is fairly close to the activation energy corresponding to grain growth exponent of 9.77 [22]. However, it has not been mentioned that over which temperature range this activation enthalpy has been calculated. Similarly, activation enthalpies of the order of 506 and 400 kJ/mol calculated using creep model in the temperature ranges of 1260–1400 and 1060–1200 °C have been reported [23,24]. However, these activation enthalpies have not been conclusively attributed to any specific element, i.e. Ba, Ti or O. Moreover, these papers are focussed on hot pressing of $BaTiO_3$ ceramics. Thus, a direct comparison may not be made but still the activation energies obtained in this research are fairly close to these activation energies in a given temperature ranges for grain growth exponents of 4.61 and 3.08 respectively. According to Lin et. al. the activation enthalpies for isothermal sintering of TiO_2-excess and BaO-excess compositions of $BaTiO_3$ are 522 ± 130 and 396 ± 16 kJ/mol in the temperature range of 1200–1300 °C and the rate controlling species in this case is barium vacancy [25]. Similar kind of research is required in case of isothermal sintering of stoichiometric compositions of $BaTiO_3$ to determine the role of each diffusing species at different stages of sintering and grain growth.

4. Conclusions

$BaTiO_3$ was synthesized by solid state reaction between $BaCO_3$ and TiO_2 at 1150 °C. XRD analysis of the powder confirmed the formation of phase pure tetragonal powder. The particle size of $BaTiO_3$ powder was of the order of 0.7 μm. In order to study grain growth kinetics of $BaTiO_3$, isothermal sintering was carried out at 1200, 1250 and 1300 °C for the time durations of 2, 4 and 6 h at each of these temperatures. Average grain size increased from 0.4 μm to 1.1 μm on increasing time and temperature of sintering. Corresponding to the temperatures of 1200, 1250 and 1300 °C, grain growth exponents obtained using phenomenological kinetic grain growth equation decreased in the order of 9.77, 4.61 and 3.08 indicating rapid coarsening with increased temperature. Grain growth exponents as high as 4.61 and 9.77 can be regarded as the result of mixed diffusion while grain growth exponent of 3.08 can be the result of pore controlled lattice diffusion. Activation energies calculated in correspondence of grain growth exponents of 9.77, 4.61 and 3.08 were 1307 ± 65, 567 ± 30 and 439 ± 20 kJ/mol respectively. Further research is required to determine the role of each diffusing species at different stages of sintering and grain growth.

Acknowledgment

Authors would like to acknowledge Sophisticated Analytical Instrumental Facility (SAIF), IIT Bombay for SEM facility used for characterization of $BaCO_3$ and TiO_2 powders. Especially, KRK would like to acknowledge Mr. Supratim Mitra, Research Scholar, Department of Metallurgical Engineering and Materials Science, IIT Bombay for fruitful discussion.

References

[1] M.M. VijatovićJ, D. Bobić, B.D. Stojanović, History and challenges of barium titanate: Part I, Science of Sintering 40 (2008) 155–165.

[2] A.K. Jha, K. Prasad, Ferroelectric $BaTiO_3$ nanoparticles: biosynthesis and characterization, Colloids and Surfaces B: Biointerfaces 75 (2010) 330–334.

[3] P. Yu, X. Wang, B. Cui, Preparation and characterization of $BaTiO_3$ powders and ceramics by the sol–gel process using organic monoacid as surfactant, Scripta Materialia 57 (2007) 623–626.

[4] P.R. Rios, T. Yamamoto, T. Kondo, T. Sakuma, Abnormal grain growth kinetics of $BaTiO_3$ with an excess TiO_2, Acta Materialia 46 (1998) 1617–1623.

[5] K.W. Kirby, B.A. Wechsler, Phase relations in barium titanate–titanium oxide system, Journal of the American Ceramic Society 74 (1991) 1841–1847.

[6] T.F. Lin, C.T. Hu, I.N. Lin, Influence of stoichiometry on microstructure and positive temperature coefficient of resistivity of semiconducting barium titanate ceramics, Journal of the American Ceramic Society 73 (1990) 531–536.

[7] D.F.K. Hennings, R. Janssen, P.J.L. Reynen, Control of liquid-phase enhanced discontinuous grain growth in barium titanate, Journal of the American Ceramic Society 70 (1987) 23–27.

[8] J.G. Fisher, B.K. Lee, S.Y. Choi, S.M. Wang, S.J.L Kang, Inhibition of abnormal grain growth in $BaTiO_3$ by addition of Al_2O_3, Journal of the European Ceramic Society 26 (2006) 1619–1628.

[9] H.Y. Lee, J.S. Kim, N.M. Hwang, D.Y. Kim, Effect of sintering temperature on the secondary abnormal grain growth of $BaTiO_3$, Journal of the European Ceramic Society 20 (2000) 731–737.

[10] H.Y. Lee, J.S. Kim, D.Y. Kim, Effect of twin-plane reentrant edge on the coarsening behavior of barium titanate grains, Journal of the American Ceramic Society 85 (2002) 977–980.

[11] Y.I. Jung, S.Y. Choi, S.J.L. Kang, Effect of oxygen partial pressure on grain boundary structure and grain growth behavior in $BaTiO_3$, Acta Materialia 54 (2006) 2849–2855.

[12] B.K. Lee, S.Y. Chung, S.J.L. Kang, Grain boundary faceting and abnormal grain growth of $BaTiO_3$, Acta Materialia 48 (2000) 1575–1580.

[13] C.S. Chen, P.Y. Chen, C.C. Chou, C. Chen, Microwave sintering and grain growth behavior of nano – grained $BaTiO_3$ materials, Ceramics International 38 (2012) S117–S120.

[14] X.I. Song, X. He, H.P. Yang, Y.X. Qu, G.Z. Qiu, Grain growth kinetics of $BaTiO_3$ nanocrystals during calcining process, Journal of Chemical Physics 21 (2008) 295–300.

[15] ASTM C 373-88, Standard test method for water absorption, bulk density, apparent porosity and apparent specific gravity of fired whiteware products, ASTM International, 1988 pp. 1–2.

[16] M.I. Mendelson, Average grain size in polycrystalline ceramics, Journal of the American Ceramic Society 52 (1969) 443–446.

[17] M.N. Rahaman, Ceramic Processing and Sintering, 2nd edition, Marcel Dekker Inc. New York, USA, pp. 800–806.

[18] T.K. Gupta, R.L. Coble, Sintering of ZnO: II Density decrease and pore growth during the final stage of the process, Journal of the American Ceramic Society 51 (1968) 525–528.

[19] T. Senda, R.C. Bradt, Grain growth in sintered ZnO and ZnO–Bi_2O_3 ceramics, Journal of the American Ceramic Society 73 (1990) 106–114.

[20] Z. Holkova, L. Pach, V. Kovar, S. Svetik, Kinetic study of Al_2O_3 sintering by dilatometry, Ceramics Silikáty 47 (2003) 13–19.

[21] A. Dias, N.D.S. Mohallem, R.L. Moreira, Solid state sintering of hydrothermal powders: densification and grain growth kinetics of nickel–zinc ferrites, Materials Research Bulletin 33 (1998) 475–486.

[22] C.V. Lewis, C.R.A. Catlow, Defect studies of doped and undoped barium titanate using computer simulation techniques, Journal of Physics and Chemistry of Solids 47 (1986) 89–97.

[23] H. Mostaghachi, R.J. Brook, Kinetics of hot-pressing of $BaTiO_3$ ceramics, British Ceramic Transactions and Journal 84 (1985) 203–206.

[24] L.A. Xue, Y. Chen, E. Cilbart, R.J. Brook, The kinetics of hot-pressing for undoped and donor-doped $BaTiO_3$ ceramics, Journal of Materials Science 25 (1990) 1423–1428.

[25] M.H. Lin, J.F. Chou, H.Y. Lu, The rate-determining mechanism in the sintering of undoped nonstoichiometric barium titanate, Journal of the European Ceramic Society 20 (2000) 517–526.